

CP Violation in Fourth Generation Quark Decays

Abdesslam Arhrib^{1,2} and Wei-Shu Hou^{1,3}

¹National Center for Theoretical Sciences, National Taiwan University, Taipei, Taiwan 10617

²Faculté des Sciences et Techniques, B.P 416 Tangier, Morocco

³Department of Physics, National Taiwan University, Taipei, Taiwan 10617

(Dated: November 2, 2018)

We show that, if a fourth generation is discovered at the Tevatron or LHC, one could study CP violation in $b' \rightarrow s$ decays. Asymmetries could reach 30% for $b' \rightarrow sZ$ for $m_{b'} \lesssim 350$ GeV, while it could be greater than 50% for $b' \rightarrow s\gamma$ and extend to higher $m_{b'}$. Branching ratios are 10^{-3} – 10^{-5} , and CPV measurement requires tagging. Once measured, however, the CPV phase can be extracted with little theoretical uncertainty.

PACS numbers: 11.30.Er, 12.15.Ff, 12.15.Lk, 12.15.Mm

Measurements of the phase angle $\sin 2\beta/\phi_1 \equiv \sin 2\Phi_{B_d}$ in $B_d \rightarrow J/\psi K^0$ and other decays are in good agreement [1] with the Kobayashi–Maskawa (KM) model [2]. This Standard Model (SM) with 3 generations predicts $\sin 2\Phi_{B_s}^{\text{SM}} \simeq -0.04$ [1] for time-dependent CP violation (TCPV) in $B_s \rightarrow J/\psi\phi$ mode, which is beyond the sensitivities at the Tevatron, and accessible only by the LHCb experiment. Any indication for a finite value at the Tevatron implies physics beyond SM (BSM).

Interestingly, both the CDF and DØ experiments reported [3] recently a large and negative value for $\sin 2\Phi_{B_s}$. Though not yet significant, the central value echoes the predictions [4] based on a fourth generation explanation of the direct CPV (DCPV) difference, $\Delta A_{K\pi} \equiv A_{B^+ \rightarrow K^+\pi^0} - A_{B^0 \rightarrow K^+\pi^-} \sim +15\%$ [1, 5], observed by the B factories. By correlations of the $b \rightarrow s$ Z -penguin and $b\bar{s} \leftrightarrow s\bar{b}$ box diagrams, a sizable 4th generation contribution to $\Delta A_{K\pi}$ would imply prominent CPV in $B_s \rightarrow J/\psi\phi$. With B_s mixing observed by CDF in 2006, a stronger prediction was made. New results on $\sin 2\Phi_{B_s}$ ($\equiv -\sin 2\beta_s$ of CDF) are eagerly awaited. To up the ante, a 4th generation could enhance the invariant CPV measure of Jarlskog [6] by a factor of 10^{15} [7], and perhaps could satisfy the CPV part of the Sakharov conditions [8] for baryogenesis in the early Universe.

The 4th generation is troubled by the electroweak precision test (EWPT) S parameter [9]. However, this severe constraint [1] is softened when one allows some t' – b' mass splitting that contributes to T parameter [10, 11]. With the LHC, we finally have a machine that can discover or rule out the 4th generation once and for all by direct search [12]. There is in fact renewed interest at the Tevatron. CDF has recently searched for $t' \rightarrow qW$ (no b -tagging) using 2.8 fb^{-1} , and for same sign dileptons [13] in $b'\bar{b}' \rightarrow t\bar{t}W^-W^+$ [12] based on 2.7 fb^{-1} data, setting the 95% C.L. limits of $m_{t'} > 311$ GeV [14] and $m_{b'} > 325$ GeV [15], respectively. Note that these limits assume predominance of the search mode. The t' and especially the b' decays could be richer.

Motivated by the BSM source of CPV, and with heightened direct search activity, we ask: What can the direct discovery of the b' and t' quarks do for the quest of

CPV? We find the best case to be flavor changing neutral current (FCNC) $b' \rightarrow s$ decays, with b' around and above the tW threshold (see Fig. 1).

The study of CPV in $b' \rightarrow s$ transitions complements the traditional agenda of BSM CPV search in the flavor sector, such as $B_s \rightarrow J/\psi\phi$, $K_L \rightarrow \pi^0\bar{\nu}\nu$, or D^0 mixing. It opens up the new chapter of very heavy flavor CPV studies. Interestingly, though of DCPV type (there is no longer the exquisite TCPV mechanism for b'), the CP conserving phases in $b' \rightarrow s$ transitions are calculable. Once measured, the CPV phase can in principle be extracted with little theoretical uncertainty.

CPV requires two interfering amplitudes $\mathcal{M} = \mathcal{M}_1 + \mathcal{M}_2$, and the CP asymmetry is

$$A_{\text{CP}} = \frac{2|\mathcal{M}_1||\mathcal{M}_2|\sin\delta\sin\phi}{|\mathcal{M}_1|^2 + |\mathcal{M}_2|^2 + 2|\mathcal{M}_1||\mathcal{M}_2|\cos\delta\cos\phi}, \quad (1)$$

which vanishes unless both the weak *and* “strong” phase differences $\phi \equiv \phi_2 - \phi_1$ and $\delta \equiv \delta_2 - \delta_1$ are nonzero. In TCPV studies, $\delta = \Delta m_B \Delta t$ is measured, allowing extraction of CPV phase ϕ . For very heavy quarks, we no longer expect meson formation because of rapid quark decay. What is left is DCPV. Fortunately, unlike B meson decays, the absorptive amplitudes of Fig. 1 are calculable, and QCD corrections perturbative.

The u quark effect in Fig. 1 is suppressed by a tiny $V_{ub}^*V_{ub'}$. Alternatively, $q = c, u$ are effectively massless, and provide a GIM subtraction to the t and t' amplitudes via $V_{qs}^*V_{qb'} + V_{ts}^*V_{tb'} + V_{t's}^*V_{t'b'} = 0$, giving

$$\mathcal{M}_{b' \rightarrow s} = V_{ts}^*V_{tb'} \Delta(t, 0) + V_{t's}^*V_{t'b'} \Delta(t', 0), \quad (2)$$

with $\Delta(a, b) = f(m_a) - f(m_b)$, and f the loop function.

Let us consider the CP conserving phase difference δ between $\Delta(t, 0)$ and $\Delta(t', 0)$. Having both t' , b' , and even

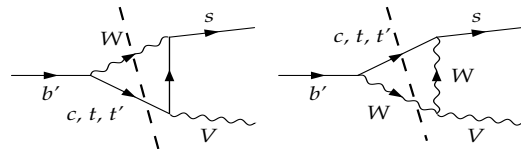


Fig. 1: $b' \rightarrow s$ loop transition, where the cut is for c and t .

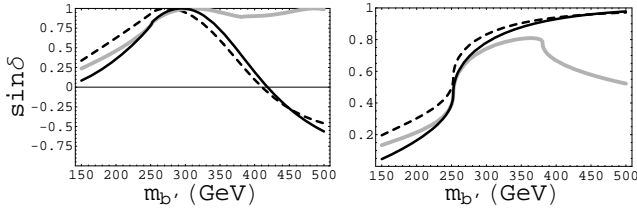


Fig. 2: CP conserving phase difference $\sin \delta$ between $\Delta(t, 0)$ and $\Delta(t', 0)$ of Eq. (2) as a function of $m_{b'}$, for $b' \rightarrow sZ_L$ (left), where Z_L is the longitudinal Z , and $b' \rightarrow s\gamma$ (right). Solid line is for $m_{t'} = m_{b'} + 50$ GeV, and grey solid (dashed) line is for $m_{t'} = 300$ (500) GeV.

the top rather heavy, enriches the strong phase difference $\sin \delta$ in Eq. (2). For b' below tW (hence $t'W$) threshold, both the t and t' effects are dispersive, the strong phase difference between GIM-subtracted t and t' contributions are subdued. But as the tW threshold (illustrated by the cut in Fig. 1) is approached, the dispersive t amplitude gets affected, and $\sin \delta$ starts to grow. Above tW threshold, the behavior of $\sin \delta$ depends on $m_{t'}$, e.g. whether it is correlated with $m_{b'}$ due to electroweak constraints. It also depends on the process.

We plot $\sin \delta$ vs. $m_{b'}$ in Fig. 2 for three t' mass scenarios, where 2(a) is for longitudinal Z emission, and 2(b) for $b' \rightarrow s\gamma$ (the transverse Z contribution to $b' \rightarrow sZ$ is similar). For the solid line of $m_{t'} = m_{b'} + 50$ GeV that satisfies the EWPT $S-T$ constraints, $\sin \delta$ rises to 1 for $b' \rightarrow sZ_L$ as one crosses the tW threshold, and stays close to 1 until it starts to drop for $m_{b'} \gtrsim 310$ GeV, changing sign for $m_{b'} \gtrsim 420$ GeV. A similar effect is seen for fixed $m_{t'} = 500$ GeV (dashed line), where $\sin \delta$ is larger than the previous case for b' below tW threshold. Thus, the flipping of sign of $\sin \delta$ is due to not crossing the $t'W$ threshold. The behavior for $b' \rightarrow s\gamma$ is different because it is a conserved current.

To illustrate $t'W$ threshold crossing, the grey solid line in Fig. 2 is for $m_{t'} = 300$ GeV. For $b' \rightarrow sZ_L$, $\sin \delta$ hardly drops above the tW threshold, and rises back to 1 after crossing the $t'W$ threshold. For all cases, we see that near and above the tW threshold, the absorptive $b' \rightarrow tW \rightarrow sV^0$ amplitude is optimal for CPV, with $\sin \delta$ of order 1. The phase difference between $V_{t's}^* V_{t'b'}$ and $V_{ts}^* V_{tb'}$ provides the CPV weak phase. We thus foresee that CPV in $b' \rightarrow sV^0$ decays is the most interesting for b' near and above the tW threshold.

What about other b' and t' loop decays? The $b' \rightarrow b$, the $t' \rightarrow t$, c , and the $t \rightarrow c$ transitions all turn out to be dominated by a single amplitude, and, according to Eq. (1), cannot generate much A_{CP} . For $b' \rightarrow b$ decays, $V_{ub}^* V_{ub'}$ and $V_{cb}^* V_{cb'}$ are rather small, so $V_{tb}^* V_{tb'} \cong -V_{t'b}^* V_{t'b'}$, hence [12] $\mathcal{M}_{b' \rightarrow b} = V_{t'b}^* V_{t'b'} \Delta(t', t)$. For $t' \rightarrow t$ transitions, m_d , m_s and m_b can be taken as 0 as compared to the weak scale, hence $\mathcal{M}_{t' \rightarrow t} = V_{tb'} V_{t'b}^* \Delta(b', 0)$, while one simply changes the CKM factor to $V_{cb'} V_{t'c}^*$ for $t^{(\prime)} \rightarrow c$ transitions. Note that the generic loop function f contains implicit external heavy mass dependence for

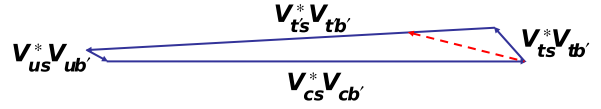


Fig. 3: The unitarity quadrangle of Eq. (3), with tilt of $V_{us}^* V_{ub'}$ exaggerated. Dashed line is explained in text.

different transitions.

So, the $b' \rightarrow s$ transitions are special. Like $b' \rightarrow b$ transitions, they are indeed loop suppressed. With a hint of possible large CPV effects in $b \rightarrow s$ transitions [3, 4, 5], which is controlled by the CKM product $V_{t's}^* V_{t'b}$, $b' \rightarrow s$ need not be far suppressed compared to $b' \rightarrow b$. From Eq. (2), we see that $b' \rightarrow s$ transitions are controlled by $V_{t's}^* V_{t'b'}$, which should not be too different in length from $V_{cb'}$ that controls the tree level $b' \rightarrow cW$ decay, as $V_{t'b'} \cong 1$ is expected. In the same way, the $b' \rightarrow b$ transitions share similar CKM dependence with $b' \rightarrow \{tW\}^*$, where the $*$ means that below threshold, the t or the W , or both, could be off-shell.

As a starting point of our numerical study, we shall use the explicit 4×4 CKM matrix from the second reference of Ref. [4], which is an illustration for $m_{t'} = 300$ GeV from a comprehensive study of $b \rightarrow s$, $s \rightarrow d$ and $b \rightarrow d$ FCNC and CPV processes. The value for $|V_{cb'}| \sim 0.116$ is rather sizable. However, if the $\Delta A_{K\pi}$ and $\sin 2\Phi_{B_s}$ indications are taken seriously, then choosing a smaller value for $|V_{t'b}|$ than 0.22 (taken in Ref. [4]), then $|V_{t's}|$ hence $|V_{cb'}|$ would only be larger. The unitarity quadrangle relevant for $b' \rightarrow s$ transitions is

$$0 = (V_{us}^* V_{ub'} + V_{cs}^* V_{cb'} + V_{ts}^* V_{tb'} + V_{t's}^* V_{t'b'}) 10^2 e^{-i66^\circ} = 0.63 e^{-i5^\circ} + 11.25 - 1.20 e^{-i42^\circ} - 11.01 e^{i4^\circ}, \quad (3)$$

and is depicted in Fig. 3. In discussions, however, we shall allow variations to illustrate the full range of possible CPV effects, e.g. the dashed line illustrates the case of a smaller $V_{cs}^* V_{cb'}$. Note that the quadrangle in Fig. 3 has the same area as the $b \rightarrow s$ quadrangle shown in Refs. [4, 7], but is somewhat squashed. This disadvantages the $b' \rightarrow s$ process for CPV purposes. To get the largest CPV asymmetry, from Eq. (1) we see that the two interfering amplitudes better have similar strength.

It is known [16] that the intertwining effects of CKM, kinematic and loop suppressions make b' decays particularly rich and interesting, especially for b' below tW threshold. The potential ‘‘cocktail solution’’ [17] can certainly evade current CDF search bounds. With the potential indication of large CPV activity in $b \rightarrow s$ transitions, $V_{t's}$ and $V_{t'b}$ could in fact be comparable in strength, further enriching the b' decay scenario. We illustrate possible branching fractions of various decay modes for b' in Fig. 4, for the low, near and above tW threshold masses of $m_{b'} = 210, 260, 340$ GeV.

The contours of A_{CP} in the plane of $m_{b'}$ and $|V_{t's}^* V_{t'b'}|$ is plotted in Fig. 5 for $b' \rightarrow sZ$ and $s\gamma$ decays, with $m_{t'} = m_{b'} + 50$ GeV. One sees clearly that the largest A_{CP} occurs around tW threshold, and for $|V_{t's}^* V_{t'b'}|$ approach-

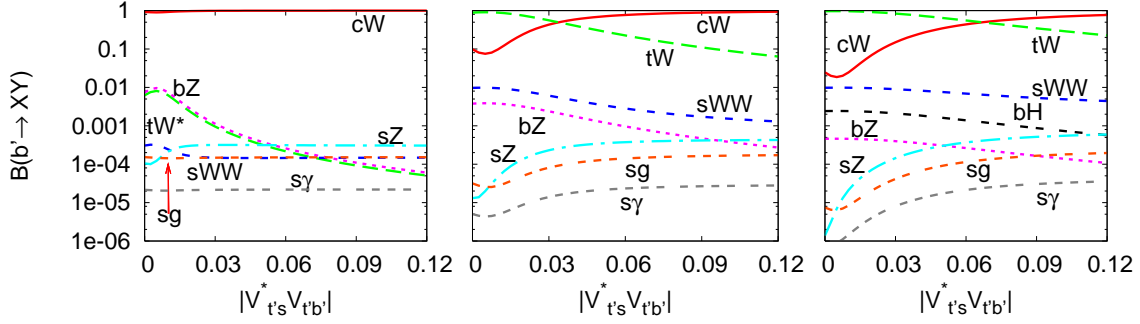


Fig. 4: Branching ratios of b' decays as a function of $|V_{t's}^* V_{t'b'}|$ with $\arg(-V_{t's}^* V_{t'b'}) = 70^\circ$, and $V_{t's}^* V_{t'b'} = -0.01 e^{i10^\circ}$, $V_{t'b'} = 0.1$, for $m_{b'} = 210$ GeV (left), 260 GeV (center) $m_{b'} = 340$ GeV (right). The CKM factors are close to, but not exactly the same as the numerical example of Ref. [4], given in Eq. (3).

ing $V_{t's}^* V_{t'b'}$ in strength. We remark that $|V_{t's}^* V_{t'b'}| \sim 0.01$ is about as large as it can get. In the limit that all rotation angles are smaller than V_{us} (Cabibbo angle), which seems to be the case, $|V_{t's}|$ remains close to the measured V_{cb} in strength, and cannot be larger than about 0.05, while $V_{t'b'} \sim 0.2$ is the bound from $Z \rightarrow b\bar{b}$ for $m_{t'} \sim 300$ GeV. For larger $m_{b'}$, $V_{t'b'}$ will have to be smaller. We see from Fig. 5 that maximal A_{CP} occurs for $|V_{t's}^* V_{t'b'}|$ not far from $|V_{t's}^* V_{t'b'}|$, as can be understood from Eq. (1). However, if Eq. (3) holds, then A_{CP} is less than -10% , smaller when away from the tW threshold. Note that the CP asymmetry flips sign for $m_{b'}$ above 440 GeV or so, which is due to the change in sign of the CP conserving phase difference $\sin \delta$, as depicted in Fig. 2.

For the $b' \rightarrow s\gamma$ case ($b' \rightarrow sg$ is qualitatively similar), because of gauge invariance, it can only be induced by a dipole transition, and the $m_t, m_{t'}$ dependence is different. As can be seen from Fig. 2, the CP conserving phase difference $\sin \delta$ turns on sharply above the tW threshold, becoming close to 1 unless the $t'W$ threshold is encountered (never the case if EWPT is respected). There is no flip of sign for $\sin \delta$, and we see from Fig. 5(b) that rather large A_{CP} can be attained for $|V_{t's}^* V_{t'b'}| \sim |V_{t's}^* V_{t'b'}|$, even towards high b' masses. But if Eq. (3) holds, then A_{CP} cannot be more than -15% , and the best mass range is above tW threshold, up to 350 GeV or so.

So far we have fixed the phase of $V_{t's}^* V_{t'b'}$ to 70° , as suggested by Ref. [4], and given in Eq. (3). To illustrate

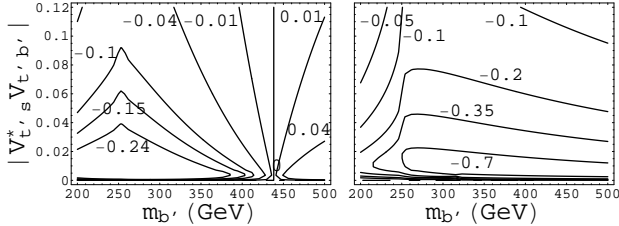


Fig. 5: Contour plots of A_{CP} for $b' \rightarrow sZ$ (left) and $b' \rightarrow s\gamma$ (right) in $m_{b'} - |V_{t's}^* V_{t'b'}|$ plane, with $m_{t'} = m_{b'} + 50$ GeV, and CKM parameters as in Fig. 4.

the dependence on this phase, we plot in Fig. 6 A_{CP} contours in the $\arg(-V_{t's}^* V_{t'b'}) - |V_{t's}^* V_{t'b'}|$ plane. Since $\arg(-V_{t's}^* V_{t'b'}) \sim 70^\circ$ is already very large, the gain for a CPV phase of $\pi/2$ is not dramatic, but A_{CP} of course vanishes if this phase turns out to be small.

We have been applying $m_{t'} = m_{b'} + 50$ GeV that respects electroweak constraints. To get a feeling of the broader behavior, in Fig. 7 we release the EWPT constraint and plot A_{CP} contours in the $m_{b'} - m_{t'}$ plane. We select the near optimal (for strength of A_{CP}) scenario of $V_{t's}^* V_{t'b'} \simeq -0.02 e^{i70^\circ}$, with our nominal $V_{t's}^* V_{t'b'} \simeq -0.01 e^{i10^\circ}$. Smaller values for $|V_{t's}^* V_{t'b'}| \simeq |V_{t's}^* V_{t'b'}|$ can give even larger CP asymmetries. Fig. 7 should be compared with Fig. 2, e.g. for $m_{t'} = m_{b'} + 50$ GeV along the illustrated dashed line (or held fixed at $m_{t'} = 300$ or 500 GeV). We see that, in case of $b' \rightarrow sZ$, the largest CP asymmetry is for $V_{t's}^* V_{t'b'}$ close to $V_{t's}^* V_{t'b'}$ in strength, with large CPV phase difference, and for $m_{t'}$ around tW threshold. For the $b' \rightarrow s\gamma$ case, the largest asymmetry occurs for $m_{b'}$ just above tW threshold, but $m_{t'}$ very heavy. These masses may not be realistic because of EWPT constraints, but they illustrate the potential range of CPV for $b' \rightarrow s$ loop transitions.

We note that, to have enhanced A_{CP} for $b' \rightarrow s$ decays, it often may not coincide with large $\sin 2\Phi_{B_s}$ in $B_s \rightarrow J/\psi\phi$. For instance, the preference for $V_{t's}^* V_{t'b'}$ close to $V_{t's}^* V_{t'b'}$, as illustrated by the red dashed line in Fig. 3, $V_{t's}^*$ has practically shrank by 1/4 to 1/5 in length,

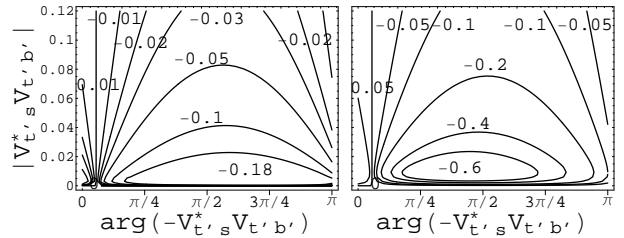


Fig. 6: A_{CP} contours for $b' \rightarrow sZ$ (left) and $b' \rightarrow s\gamma$ (right) in $\arg(-V_{t's}^* V_{t'b'}) - |V_{t's}^* V_{t'b'}|$ plane, with $m_{b'} = 340$ GeV and $m_{t'} = m_{b'} + 50$ GeV, and $V_{t's}^* V_{t'b'} = -0.01 e^{i10^\circ}$, $V_{t'b'} = 0.1$.

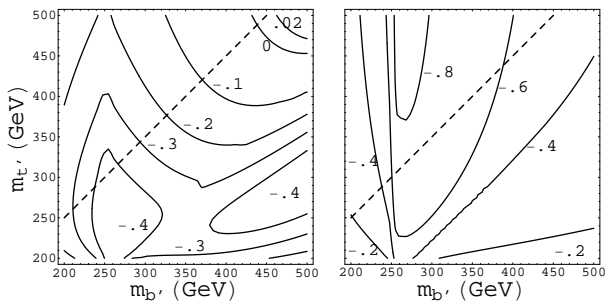


Fig. 7: A_{CP} contours for $b' \rightarrow sZ$ (left) and $b' \rightarrow s\gamma$ (right) in $m_{b'}-m_{t'}$ plane, for $V_{t's}^*V_{t'b'} \simeq -0.02 e^{i70^\circ}$, $V_{ts}^*V_{tb'} \simeq -0.01 e^{i10^\circ}$. The dashed line is for $m_{t'} = m_{b'} + 50$ GeV.

so $\sin 2\Phi_{B_s}$ may not be as strong as the current Tevatron central value, but would still be very interesting for LHCb. Likewise, $K_L \rightarrow \pi^0 \nu \bar{\nu}$ and CPV in D^0 mixing are open questions. Thus, the impact of a 4th generation on BSM CPV effects is quite an open question, to be pursued at multiple fronts.

We see that $A_{CP}(b' \rightarrow sZ)$ can in principle go up to 30%–40%, especially if $m_{t'}$, $m_{b'} \lesssim 350$ GeV or so (and $m_{b'} > m_{t'}$ would be better). Larger asymmetries are possible for $b' \rightarrow s\gamma$, and extending to high $m_{b'}$. But what about the current CDF search bounds? Note that these assume either $t' \rightarrow qW$ (no b -tagging) or $b' \rightarrow tW$ to be 100%. As illustrated in Fig. 4, for $m_{b'}$ in the range from tW threshold to 350 GeV or so, branching ratios depend on $V_{cb'}$ ($V_{t's}^*V_{t'b'}$ for $b' \rightarrow s$) and $V_{tb'}$ ($V_{t'b}^*V_{t'b'}$ for $b' \rightarrow b$) for the $b' \rightarrow cW$ and $b' \rightarrow tW$ processes, respectively, and may still evade current bounds. For example, the smaller value of $V_{t's}^*V_{t'b'}$ that drives up A_{CP} , as illustrated by the red dashed line of Fig. 3, implies smaller $b' \rightarrow cW$ and $b' \rightarrow s$ rates. Of course, $V_{tb'}$ could be smaller as well, but this could be compensated by a larger b' mass than in Fig. 4(a). What is not sufficiently illustrated in Fig. 4 is that $V_{cb'}$ can be suppressed, but with $V_{t's}^*V_{t'b'}$ less suppressed (we have treated the reverse

case). This is because of CKM unitarity (similar to $V_{td} \neq 0$ in $V_{ub} \rightarrow 0$ limit), and again illustrates the potential richness of multiple decay channels for b' , which is best studied with LHC data in the near future.

Besides A_{CP} and branching fraction, the actual measurability of CPV in $b' \rightarrow s$ decays also requires tagging. Let us take $b'\bar{b}'$ production cross section ~ 40 pb for $m_{b'} \sim 300$ GeV with 14 TeV running of LHC, and a typical $b' \rightarrow sZ$ branching ratio of order a few $\times 10^{-4}$. The tagging efficiency for the other \bar{b}' (gaining a factor of two in a $b'\bar{b}'$ event) is hard to estimate at present, and would depend on $b' \rightarrow cW$ vs $\{tW\}^{(*)}$ fractions. With 100 fb^{-1} , we very roughly infer that a 10% asymmetry may be reachable with 3σ statistical significance. The $b' \rightarrow s\gamma$ mode may be more promising. Though typically 1/10 the $b' \rightarrow sZ$ rate, there is no need for $Z \rightarrow \ell^+\ell^-$ reconstruction, and the asymmetry could be 50% or larger. The $b' \rightarrow sg$ would suffer more background for CPV studies because of lack of distinct signature, and would be less useful. The situation may be better for an e^+e^- linear collider environment.

We note that if large $\sin 2\Phi_{B_s}$ is observed, hence something closer to Eq. (3) or Fig. 3 is realized, it would imply smaller A_{CP} . If $\sin 2\Phi_{B_s}$ is found positive, the A_{CP} s discussed here would flip in sign. Note also that $b' \rightarrow sWW$ mode could also exhibit CPV, but the asymmetry is suppressed by Γ_t/m_t or Γ_W/M_W and small.

In conclusion, the best scenario for CPV studies at high energy collider is for $b' \rightarrow s$ decays. One would first have to discover the 4th generation, preferably around 300 GeV or so. After sorting out the dominant decays, one would have to identify $b' \rightarrow sZ$ or $b' \rightarrow s\gamma$ channels, and then tag the other \bar{b}' . The study of CPV in b' decays would demand more than 100 fb^{-1} at the LHC. But if measured, one could extract the CPV phase, since the CP conserving phase is calculable.

Acknowledgement. We thank the National Science Council of R.O.C. for partial support.

-
- [1] C. Amsler *et al.* [Particle Data Group], Phys. Lett. **B667**, 1 (2008).
[2] M. Kobayashi and K. Maskawa, Progr. Theor. Phys. **49** (1973) 652.
[3] T. Aaltonen *et al.* [CDF Collaboration], Phys. Rev. Lett. **100**, 161802 (2008); V.M. Abazov *et al.* [DØ Collaboration], *ibid.* **101**, 241801 (2008).
[4] W.S. Hou, M. Nagashima and A. Soddu, Phys. Rev. Lett. **95** (2005) 141601; Phys. Rev. D **72** (2005) 115007; *ibid.* **D 76** (2007) 016004.
[5] S.W. Lin, Y. Unno, W.S. Hou, P. Chang *et al.* [Belle Collaboration], Nature **452**, 332 (2008).
[6] C. Jarlskog, Phys. Rev. Lett. **55**, 1039 (1985).
[7] W.S. Hou, Chin. J. Phys. **47** (2009) 134.
[8] A.D. Sakharov, Pis'ma Zh. Eksp. Teor. Fiz. **5**, 32 (1967).
[9] $N_\nu \cong 3$ on the Z peak is muted by the observation of neutrino oscillations, which implies a BSM mass scale.
[10] G.D. Kribs, T. Plehn, M. Spannowsky, and T.M.P. Tait, Phys. Rev. D **76**, 075016 (2007).
[11] B. Holdom *et al.*, arXiv:0904.4698 [hep-ph].
[12] A. Arhrib and W.S. Hou, JHEP **07**, 009 (2006).
[13] The signature was studied for early data search in CMS Physics Analysis Summary, CMS PAS EXO-08-09.
[14] T. Aaltonen *et al.* [CDF Collaboration], Phys. Rev. Lett. **100**, 161803 (2008); and <http://www-cdf.fnal.gov>.
[15] CDF public note CDF/PHYS/EXO/PUBLIC/9759.
[16] W.S. Hou and R.G. Stuart, Phys. Rev. Lett. **62**, 617 (1989); Nucl. Phys. B **320**, 277 (1989).
[17] A. Arhrib and W.S. Hou, Phys. Rev. D **64**, 073016 (2001).